

Current-controlled nanotube growth and zone refinement

K. Jensen,^{a)} W. Mickelson, W. Han, and A. Zettl^{b)}

Department of Physics, University of California at Berkeley, Berkeley, California 94720 and
Materials Sciences Division, Lawrence Berkeley National Laboratory, Berkeley, California 94720

(Received 21 December 2004; accepted 9 March 2005; published online 20 April 2005)

We describe methods by which the growth of a single carbon nanotube (CNT) can be precisely controlled by an electrical current. In one method a CNT is grown to a predetermined geometry inside another nanotube, which serves as a reaction chamber. Another method allows a preexisting marginal-quality multiwall CNT to be zone refined into a higher-quality multiwall CNT by driving a catalytic bead down the length of the nanotube. In both methods, the speed of nanotube formation is adjustable, and the growth can be stopped and restarted at will. © 2005 American Institute of Physics. [DOI: 10.1063/1.1920427]

Carbon nanotubes (CNTs) are remarkable materials with interesting mechanical, electrical, and thermal properties.^{1–3} These properties are sensitive to geometrical details, which depend intricately on the method of nanotube growth. As such, much effort has been devoted to studying CNT synthesis and growth mechanisms. Numerous methods presently exist for CNT production.^{4–6} Unfortunately, none of these bulk synthesis methods affords truly controlled growth, whereby a CNT can be grown at a precisely determined rate with a preselected diameter, length, and defect concentration. We here present two reaction methods by which the growth of a single CNT can be precisely controlled using an electrical current. In the first method, a CNT grows inside a preformed nanotube reaction chamber. In the second closely related method, a preexisting marginal-quality multiwall CNT is zone refined into a higher-quality multiwall CNT.

Our experimental configuration exploits the well-known critical role transition metal catalysts play in CNT growth as well as the ability to transport metals along^{7,8} preformed nanotubes. Multiwall CNTs containing cobalt catalyst nanoparticles in their interior were synthesized through the pyrolysis of cobaltocene.⁹ A mat of cobalt-filled nanotubes was then glued to a platinum wire with conducting silver epoxy and mounted to a custom-made piezo-controlled nanomanipulation stage, operated inside a transmission electron microscope (TEM). Inside the TEM, the free end of a single nanotube was approached and contacted with an etched tungsten tip, thus completing a circuit between the grounded tungsten tip and the sample that can be held at an arbitrary voltage.

Figure 1 shows a schematic of our experimental setup and distinguishes the two modes of operation. Figure 1(a) shows what we term the “ink reservoir” method of nanotube growth. A cobalt catalyst nanoparticle, initially containing dissolved carbon (the “ink”), is confined within the interior of a preformed nanotube, which serves as the reaction chamber. An electrical current I runs through the reaction chamber, causing the catalyst particle to melt and move to the right at velocity v , streaming out a newly formed CNT in its wake. The outer diameter of the new CNT is dictated by the inner diameter of the reaction chamber, and the speed at which the catalyst particle ejects the new CNT is controlled

by I . CNT growth ceases when the cobalt catalyst particle exhausts its feedstock of dissolved carbon. Figure 1(b) shows the “zone refinement” configuration. A preformed nanotube of marginal quality contains a cobalt catalyst nanoparticle, which encompasses its entire cross section. An electrical current I again runs axially through the nanotube, causing the cobalt nanoparticle to melt and move to the right. In doing so, the original nanotube is consumed by the catalyst nanoparticle and a higher-quality CNT is grown and ejected from the trailing end. In this continuous process there is no carbon feedstock limitation and the entire original nanotube can be zone refined into a higher-quality CNT.

We first examine the ink reservoir method of controlled CNT growth. Figure 2 shows a time sequence of TEM video images depicting the movement of a cobalt catalyst particle through the core of the nanotube reaction chamber. The grounded tungsten tip contacts the right side of the nanotube while the sample side is held at a negative potential (both out of view). With increasing I , Joule heating melts the catalyst particle (the dark cigar-shaped object), and electric field effects generate a force that displaces it towards the anode on

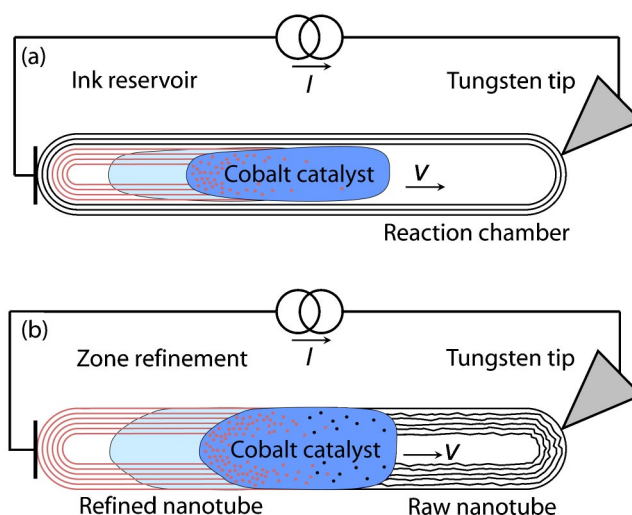


FIG. 1. (Color online). Schematic diagrams of the two modes of operation. (a) The ink reservoir method. As the catalyst moves, carbon initially dissolved in the catalyst particle (the “ink”) precipitates out and forms a new high-quality CNT (red). (b) The zone refinement method. The catalyst particle continuously refines the raw, defective nanotube on the right (black) into a higher-quality nanotube on the left (red).

^{a)}Electronic mail: kjensen@alum.mit.edu

^{b)}Electronic mail: azettl@socrates.berkeley.edu

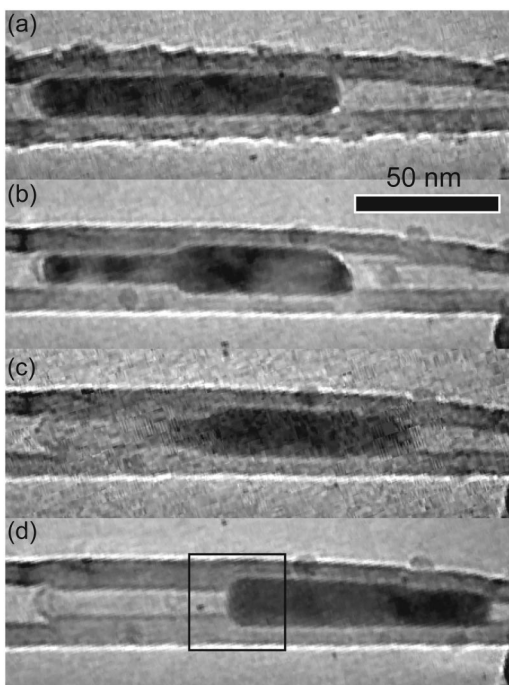


FIG. 2. A time sequence of TEM video images showing the controlled movement of a cobalt catalyst particle.

the right. In Fig. 2(b) the current is ramped to $60 \mu\text{A}$, and the catalyst particle distorts in shape and begins moving to the right. Further increasing I increases the velocity v of the catalyst particle. Between Figs. 2(c) and 2(d), both with $I = 130 \mu\text{A}$, the catalyst travels 68 nm in less than 0.1 s. As the catalyst particle moves to the right within the nanotube reaction chamber, it ejects behind it a new multiwall CNT.

Figure 3 shows a high-resolution TEM micrograph of the outlined area in Fig. 2(d) taken after the catalyst particle was frozen in place. In contrast to the reaction chamber

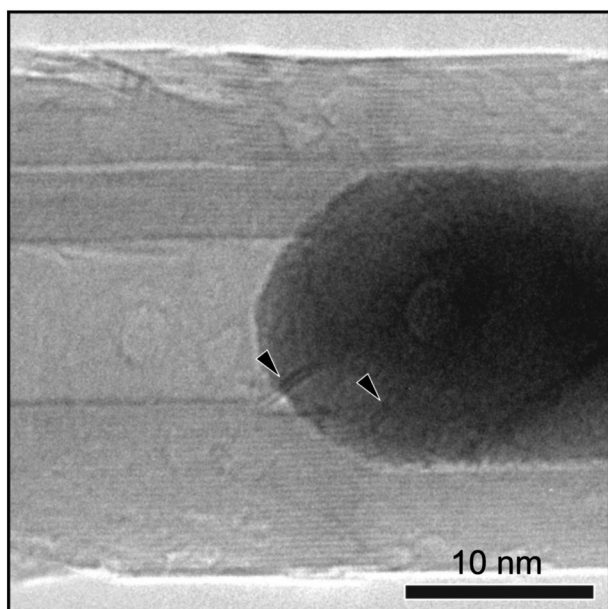


FIG. 3. TEM micrograph of a high-quality multiwall CNT growing within the core of a larger nanotube reaction chamber. This is the area outlined in Fig. 2(d). The image clearly shows the formation of a new, high-quality 11-wall CNT streaming from the end of the catalyst particle. Arrows mark multiple double graphene sheets emerging from the catalyst.

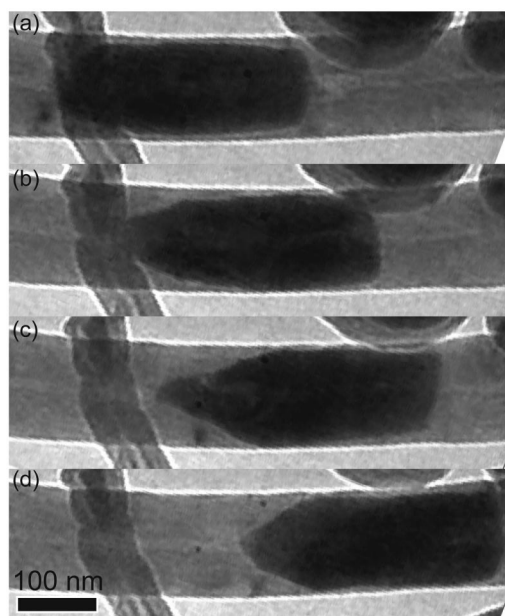


FIG. 4. A time sequence of TEM video images showing a cobalt catalyst particle cannibalize a raw nanotube to its right and reform a CNT to its left as it moves toward the anode.

nanotube, which has defect-filled walls, the newly formed CNT ejected from the catalyst particle has virtually perfect walls with no detectable defects, even near the interface with the reaction chamber. Essentially a snapshot of catalytic CNT growth, this figure contains a wealth of information pertinent to nanotube formation. In particular, the figure shows multiple double graphene sheets emerging from the catalyst particle at an angle to the walls of the newly formed CNT. Interpreting the double graphene sheets as portions of nanotube shells, we find that, in this growth process, CNT walls are laid down or “paved” on top of each other from the outside in, rather than simply being ejected from the catalytic particle simultaneously. Atomic resolution videos capturing the synthesis of multiwall CNTs in action have obvious implications for the thermodynamic analysis of nanotube synthesis.

In the ink reservoir method of CNT formation, growth ceases when the catalyst particle depletes its feedstock of dissolved carbon. For the new CNT shown in Fig. 2, growth was limited to about 70 nm. The volume of the catalyst particle decreases as it expels the new CNT (by 760 nm^3 from the initial volume of $1.6 \times 10^4 \text{ nm}^3$). Attributing the entire volume loss to carbon, we estimate that the catalyst particle initially contained approximately 5.9 at. % carbon.

We next examine the zone refinement method of controlled CNT growth described in Fig. 1(b). Figure 4 shows a time sequence of TEM video images taken at 10-s intervals depicting a catalyst particle refining a multiwall carbon nanotube. A constant current of $240 \mu\text{A}$ runs through the nanotube. The catalyst particle encompasses practically the entire diameter of the nanotube, and as it advances towards the anode (out of view to the right), it cannibalizes the raw nanotube at its front. A light band running through the center of the particle indicates a radial carbon concentration gradient in the particle resulting from the fact that no carbon is absorbed from the hollow nanotube core. The absorbed carbon is reformed into a new, higher-quality CNT at its rear. Over the course of the experiment, the resistance of the en-

ture nanotube (raw and reformed) is found to decrease by 6% following the advance of the catalyst along the full 3- μm length of the nanotube. Hence, the refined nanotube has an enhanced electrical conductance, which is consistent with a decreased defect concentration. In contrast to the ink reservoir method, in the zone refining method a constant supply of carbon ingested at the head of the catalyst particle allows for essentially unlimited dissolution and precipitation of CNTs.

The carbon supply's effect on transport suggests that the electromigration of carbon in cobalt drives the motion. Previous experiments have shown that carbon ions move toward the cathode in cobalt.¹⁰ Here the direct electrostatic force on the carbon ions dominates over the "electron wind" force resulting from the momentum transfer between electrons and ions.¹¹ As a result a carbon concentration gradient develops across the catalyst particle. Eventually, the side of the particle near the cathode becomes supersaturated with carbon causing the carbon to precipitate. The maximum carbon concentration, n_{max} , may be calculated from the 12.75 at. % carbon that cobalt, in its liquid state near the melting point, can accommodate.¹² When the carbon precipitates, it forms new concentric nanotube shells that displace the cobalt, as demonstrated in Fig. 2(b). To minimize surface energy, molten cobalt will minimize contact surface area with the nanotube. Thus, as shown in Figs. 2(c) and 2(d), surface tension forces the catalyst particle out of the region narrowed by new CNT formation, and the catalyst particle moves forward.

To test our model, we estimate the current density necessary to initiate movement by calculating the electric field required to increase the carbon concentration to n_{max} on the side of the particle near the cathode. The carbon concentration across the cobalt particle in the steady state is given by combining the Nernst-Einstein equation with the diffusion equation to yield: $n(x) = n(0) \exp(-Z^0 e |E| x / kT)$ where n is the ion concentration, Z^0 is the effective valence of the ion, e is the charge of an electron, \vec{E} is the electric field, k is the Boltzmann constant, and T is the temperature.¹¹ According to our model, carbon will precipitate and the particle will move when $n(0) = n_{\text{max}}$. For the particle displayed in Fig. 2(a), assuming the precipitation of all the initial carbon is respon-

sible for the noted volume change, we find that the mean ion concentration, $\bar{n} = 5$ ions/nm³. Thus, with $Z^0 = 10$,¹¹ $n_{\text{max}} = 10$ ions/nm³, and $T = 1000$ K,^{13,14} we determine $|\vec{E}| \approx 1.3 \times 10^{-4}$ V/nm. Assuming all current passes through the cobalt catalyst particle and using the resistivity of pure molten cobalt ($\rho_{\text{Co}} = 8.7 \times 10^{-7}$ Ω m),¹⁵ we calculate that $I \approx 20$ μA , the same magnitude as experimentally observed values.

Our technique offers the opportunity both to study nanotube growth with atomic resolution in a controllable manner and to fine-tune the parameters of nanotube formation.

We thank V. Crespi for helpful interactions. This work was supported by the Director, Office of Energy Research, Office of Basic Energy Sciences, Division of Material Sciences, of the U.S. Department of Energy under Contract No. DE-AC03-76SF00098.

¹P. Poncharal, Z. L. Wang, D. Ugarte, and W. A. de Heer, *Science* **283**, 1513 (1999).

²M. Bockrath, D. H. Cobden, J. Lu, A. G. Rinzler, R. E. Smalley, T. Balents, and P. L. McEuen, *Nature (London)* **397**, 598 (1999).

³J. Hone, M. Whitney, C. Piskoti, and A. Zettl, *Phys. Rev. B* **59**, R2514 (1999).

⁴T. W. Ebbesen and P. M. Ajayan, *Nature (London)* **358**, 220 (1992).

⁵W. Z. Li, S. S. Xie, L. X. Qian, B. H. Chang, B. S. Zou, W. Y. Zhou, R. A. Zhao, and G. Wang, *Science* **274**, 1701 (1996).

⁶T. Guo, P. Nikolaev, A. Thess, D. T. Colbert, and R. E. Smalley, *Chem. Phys. Lett.* **243**, 49 (1995).

⁷B. C. Regan, S. Aloni, R. O. Ritchie, U. Dahmen, and A. Zettl, *Nature (London)* **428**, 924 (2004).

⁸K. Svensson, H. Olin, and E. Olsson, *Phys. Rev. Lett.* **93**, 145901 (2004).

⁹B. C. Satishkumar, A. Govindaraj, R. Sen, and C. N. R. Rao, *Chem. Phys. Lett.* **293**, 47 (1998).

¹⁰P. S. Ho and T. Kwok, *Rep. Prog. Phys.* **52**, 301 (1989).

¹¹J. N. Pratt and R. G. R. Sellors, *Electrotransport in Metals and Alloys*, Diffusion and Defect Monograph Series, No. 2 (Trans Tech SA, Riechen, 1973).

¹²M. Hansen, R. P. Elliott, F. A. Shunk, and I. R. Institute, *Constitution of Binary Alloys*, Metallurgy and Metallurgical Engineering Series, 2nd ed. (McGraw-Hill, New York, 1958), prepared with the cooperation of Kurt Anderko. Translation and revision of *Der Aufbau der Zweistofflegierungen*.

¹³P. Buffat and J. P. Borel, *Phys. Rev. A* **13**, 2287 (1976).

¹⁴O. P. Krivoruchko and V. I. Zaikovskii, *Mendeleev Commun.* **8**, 97 (1998).

¹⁵T. Fujiwara, *J. Phys. F: Met. Phys.* **9**, 2011 (1979).